Persistence of uranium emission in laser-produced plasmas

N. L. LaHaye, S. S. Harilal,[a] P. K. Diwakar, and A. Hassanein
Center for Materials Under Extreme Environment, School of Nuclear Engineering, Purdue University, West Lafayette, Indiana 47907, USA

(Received 13 March 2014; accepted 13 April 2014; published online 22 April 2014)

Detection of uranium and other nuclear materials is of the utmost importance for nuclear safeguards and security. Optical emission spectroscopy of laser-ablated U plasmas has been presented as a stand-off, portable analytical method that can yield accurate qualitative and quantitative elemental analysis of a variety of samples. In this study, optimal laser ablation and ambient conditions are explored, as well as the spatio-temporal evolution of the plasma for spectral analysis of excited U species in a glass matrix. Various Ar pressures were explored to investigate the role that plasma collisional effects and confinement have on spectral line emission enhancement and persistence. The plasma-ambient gas interaction was also investigated using spatially resolved spectra and optical time-of-flight measurements. The results indicate that ambient conditions play a very important role in spectral emission intensity as well as the persistence of excited neutral U emission lines, influencing the appropriate spectral acquisition conditions. © *2014 AIP Publishing LLC*. [http://dx.doi.org/10.1063/1.4873120]

I. INTRODUCTION

The detection of special nuclear materials (SNMs), such as uranium and thorium, is of particular interest to many agencies around the world. Many of the applications require a safe, simple, easy-to-use, portable method that is able to accurately identify and detect low concentrations of the elements of interest.[1,2] There are several advantages for using laser ablation (LA) for nuclear material detection, which include minimal sample preparation, near instantaneous detection, and isotope detection. Well known laser ablation methods used for elemental and isotope detection are LA-inductively coupled plasma-mass spectrometry (LA-ICP-MS),[3,4] LA-laser absorption spectroscopy (LA-LAS),[5] and LA-optical emission spectroscopy (LA-OES). In LA-OES, commonly called laser-induced breakdown spectroscopy (LIBS), a laser is focused down onto a target to create plasma and the spectral emission from the produced plasma is detected and analyzed. One of the main advantages of OES is noninvasive and near-instantaneous detection and identification of elements in the sample. The capability of remote analysis is another advantage of LA-OES for nuclear safeguard applications, in which suspicious materials cannot always be taken to a lab for analysis.

Though SNMs such as spent fuel rods and weapons-grade uranium are not readily available for analysis, safer surrogate materials can be used to get a baseline for optimal detection conditions. NIST has standards available with trace and ultra-trace concentrations of U and Th, while some glass filters contain U in 1%–10% concentrations. Additionally, U-containing ores are also available. Even though these surrogate materials are not of the exact composition as the SNMs of interest, they are similar enough to provide information into the potential behavior of SNMs under the same ablation and detection conditions.

Investigations into the feasibility of OES for U detection have used both SNMs and surrogate materials,[6–8] including uranium oxide powders and pelletized versions of said powders.[9] Experiments have primarily used spatially integrated optical emission collection methods, e.g., with a fiber optic cable. Trace concentrations of U have been detected, with detection limits determined to be in the parts per million (ppm) range.[10–12] Various ambient environments have also been explored for detection of bulk SNMs, including air and Ar at various pressures.[13] As U has a very complex atomic structure with closely packed emission lines, high spectral resolution is a crucial figure of merit. The presence of ambient pressure during plasma generation can help to enhance line intensity and persistence through collisional and confinement effects; however, its presence may also lead to superficial effects such as line broadening thereby hindering the identification of already crowded spectra. Hence more comprehensive studies are needed to understand the role of the ambient gas and pressure on high-Z element material (e.g., U).

Using spectroscopy, isotopic shifts can also be measured, allowing for U enrichment estimations to show whether the sample is depleted (natural) U, low-enriched uranium (LEU) used in nuclear reactors, or weapons-grade high-EU (HEU).[10] These shifts have been simulated as well.[14] However, spectral separation of isotopic shifts ($\Delta \sim 20$ pm in wavelength) requires the use of high-resolution spectrographs. Portable LA-OES systems with high-resolution spectrographs have been investigated for field monitoring applications, where knowledge of U enrichment factors is necessary.[15,16] So far, experiments have been comprised of spatially and temporally integrated measurements, giving no information about the U plasma evolution and optimal spatio-temporal collection of emission from U species in the plasma. Information on plasma spatial and temporal evolution is not only important for the LIBS and LA-OES community; laser absorption techniques

[a]Author to whom correspondence should be addressed. Electronic address: hari@purdue.edu

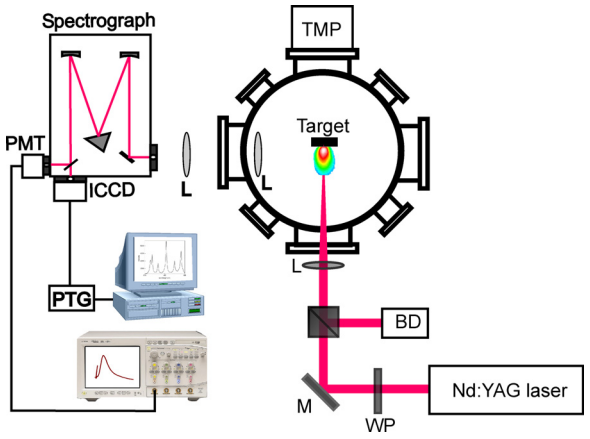

FIG. 1. Experimental setup for laser-plasma spectroscopy. The spectrograph can divert dispersed light either to the ICCD camera for analysis of a range of wavelengths or to a PMT for OTOF studies of an excited emission line. TMP: turbo-molecular pump; ICCD: intensified charge-coupled device; PTG: programmable timing generator; L: lens; M: mirror; BD: beam dump; WP: half-waveplate.

require information on characteristic plasma evolution as well for proper excitation.[5]

This work presents a novel determination of the spatio-temporal evolution of plasmas created by laser ablation of uranium-containing samples. The ablation conditions were varied, including laser energy and ambient gas pressure, to get the optimal U line emission intensity. The persistence of the plasma is of great importance to ensure that the majority of line emission is being captured within the spectral time integration window. Spatially and temporally resolved spectral studies and time-of-flight emission spectroscopy of excited uranium atoms were carried out, which demonstrated the expansion hydrodynamics as well as U species persistence. These results combined to provide insight into U line excitation and the optimum operating pressure conditions for detection of U using OES.

II. EXPERIMENTAL

A schematic of the experimental set-up is given in Fig. 1. The fundamental wavelength (1064 nm) of a pulsed Nd:YAG laser with 6 ns FWHM was used for excitation and ablation of the target containing U. The laser was set to a repetition rate of 2 Hz to avoid crater effects due to target drilling, with a combination of a half-waveplate and polarizing cube used to attenuate the laser energy in the range of 25–120 mJ. The laser beam was focused down using a plano-convex lens of focal length 40 cm. The laser spot was kept to a diameter of ~1 mm. The target used contained 1.3% U in a glass matrix (SiO_2 and CaO). The target was mounted on a motorized translation stage to avoid target cratering effects.

Two additional plano-convex lenses of focal length 40 cm focused the plasma emission onto the introduction slit of a 0.5 m Czerny-Turner spectrograph, equipped with a high resolution grating with 1800 grooves/mm for dispersion. The resolution of the spectrograph is ~0.025 nm. The slit width was maintained at 30 μm so as to image a very narrow region of the plasma for better spatial resolution. The dispersed light from the spectrograph was diverted to either an ICCD camera for detection of a range of wavelengths or a photomultiplier tube (PMT) for optical time-of-flight (OTOF) detection of emission from a particular wavelength. When using the ICCD camera for detection, a gate delay of 1 μs and gate width of 20 μs were used for spatial analysis, whereas for temporal analysis, the gate delay was varied from 0 to 50 μs with gate width 10% of the gate delay.

All experiments were performed within a vacuum chamber, capable of pressure ranges between atmospheric pressure and $\sim 10^{-5}$ Torr. Argon was chosen as the ambient gas due to its inert properties; a reactive ambient gas such as air could affect plasma emission properties due to quenching;[17] moreover, uranium is oxygen-reactive, causing increased background emission in the presence of air.[13] Table I lists the U I lines identified in the analyzed emission region (350 nm to 370 nm, chosen due to the absence of interference from matrix emission lines) and their spectroscopic parameters, obtained from Ref. 18; the U I 356.18 nm line was used for studying analytical merits of spectral emission and OTOF studies.

III. RESULTS AND DISCUSSION

LA involves the process of interaction of a high power laser with a solid target. The LA process contains three main stages: (i) evaporation of the target material, (ii) interaction of the evaporated cloud with incident laser beam resulting in cloud heating and plasma formation, and (iii) expansion and rapid cooling of the plasma.[19] The properties of laser-ablated plasma are highly dynamic, and the fundamental plasma quantities vary radically in time and space, which, in turn, affect the populations of various species in the ground and excited levels. We performed spatial and temporal analysis of visible emission from the U-containing plasma. Observations were made of the plasma created by the interaction of the laser beam with the target in a direction normal to the target surface. An understanding of the evolution of

TABLE I. A list of U I lines identified in the spectral window detected along with its spectroscopic parameters.

Species	Wavelength (nm)	Upper energy level (cm^{-1})	Lower energy level (cm^{-1})	log (gf)
U I	353.97	32044.130	3800.829	0.08
U I	355.53	28118.841	0	0.057
U I	356.18	28067.646	0	0.3
U I	358.48	27886.992	0	0.712
U I	358.98	31649.685	3800.829	0.05
U I	363.82	31279.129	3800.829	0.566
U I	367.05	34881.927	7645.645	0.475

U-containing plasmas under various conditions is crucial for optimization of many analytical techniques, including LIBS, LA-ICP-MS, and LA-LAS. The effect of laser excitation energy, ambient gas pressure, distance from the target, and temporal evolution on U-containing plasmas was studied in an effort to better understand the plasma evolution, species persistence, and emission properties.

A. Laser excitation energy effects

Laser excitation energy plays an important role in plasma formation and emission properties. The spectral emission in the range of 350–370 nm as a function of laser excitation energy can be seen in Fig. 2, taken 2 mm from the target surface with Ar as ambient gas at 100 Torr. These time-integrated spectra were taken with a delay time of 1 μs to avoid the initial high continuum/background emission and a gate width of 20 μs due to the long plasma persistence. The laser energy was varied from 25 mJ up to 120 mJ. Multiple U lines were identified (Table I) with good resolution and intensity, despite the closely packed line emission. Though emission intensity increases as laser energy increases, continuum/background emission also increases; higher laser energy causes more ionization within the plasma, which leads to more free electrons contributing to the continuum. Additionally, uranium's multi-electron system means that the spectral line emission is very crowded, with significant line overlapping. Chinni *et al.*[13] attributed increased background emission to overlapping of the high density U lines and observed that the background decays with the same behavior as both neutral and ionic line emission, indicating that the background emission is increased by line emission itself. However, our OTOF studies showed that (given in Sec. III D), there exists strong continuum radiation in U containing plasmas. Therefore, background is defined as a combination of continuum emission and overlapping U lines.

An important consideration in spectroscopy is the intensity of the line emission. Due to its high intensity and clear separation from other lines, the U I line at 356.18 nm was chosen for the following analysis. Fig. 2 shows both the line intensity and background increased with laser energy. For analytical applications, signal-to-noise (S/N) and signal-to-background (S/B) ratios are important. In Fig. 3, the background-subtracted line intensity and signal to background ratio are plotted versus laser energy for the U I 356.18 nm line. The spectra were taken 2 mm from the target with 100 Torr Ar gas environment. Very little U spectral intensity is observed for 25 mJ ablation and most of the identified lines originated from the glass matrix sample (Ca and Si). It indicates that higher laser energy is required for exciting U species in the sample. This can be understood by considering the low U concentration in the glass matrix (1.3%). The spectral intensity increases rapidly with laser energy; above 80 mJ, the emission intensity slightly increases and approaches a plateau due to a balance between increased continuum emission from plasma heating versus increased line emission. The optimum laser energy resides in this plateau region, as small changes in laser energy will not cause large changes in signal. The near plateau region, where the signal increase balances with the continuum increase can also be seen in the signal to background ratio. Very low line emission is also observed at 25 mJ in the S/B ratio (where no observed signal would result in a S/B of 1, at 25 mJ, the S/B is ~1.1), with a rapid increase up to 60 mJ. The S/B then slowly falls off and equilibrates for the same plateau region that is observed in intensity. This indicates that the excess laser energy is not improving the S/N or S/B ratios. Saturation of line intensity could be due to plasma screening, which occurs when the plasma reaches critical density and has a laser excitation wavelength proportionality of λ^{-2}. As the wavelength used here is 1064 nm, plasma screening occurs at an earlier time than with shorter laser wavelengths. Because of these results, 100 mJ was chosen as the energy for the rest of the experiments. This energy resides in the line emission plateau region, so the emission intensity is high and error introduced by any energy fluctuations is minimal, while still maintaining a good S/B ratio.

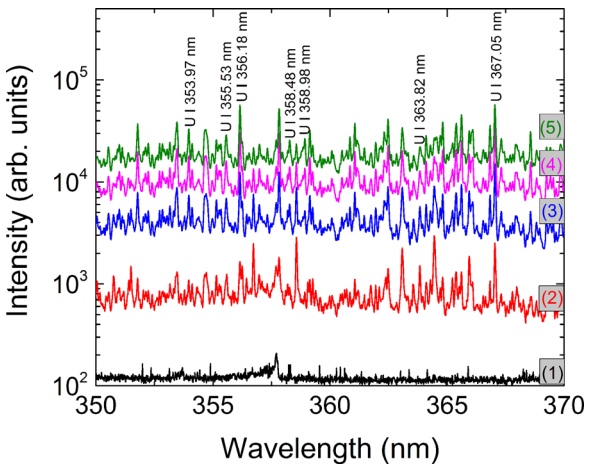

FIG. 2. Spectra obtained for laser energies between 25 mJ and 120 mJ, taken 2 mm from the target (1) 25 mJ, (2) 40 mJ, (3) 60 mJ, (4) 80 mJ, and (5) 120 mJ. Though line emission increases with increasing energy, background emission also increases. The spectral measurements were taken with an ambient Ar pressure ~100 Torr.

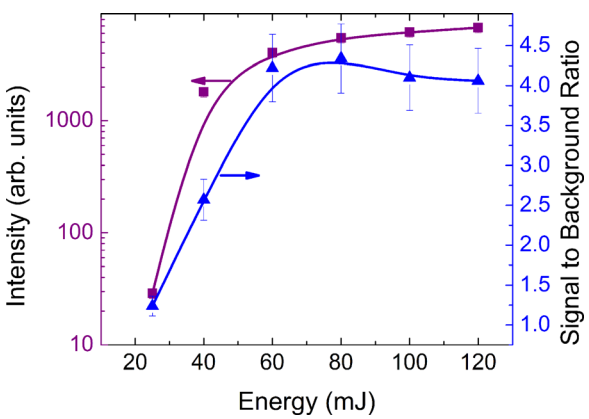

FIG. 3. Intensity and signal to background ratio of the U I 356.18 nm line versus laser energy, taken 2 mm from the target. Intensity approaches a plateau for energies 80–120 mJ. S/B ratio increases rapidly, peaks between 60 and 90 mJ, then decreases slowly due to increased background emission. The measurements were performed with ambient pressure of 100 Torr Ar.

B. Ambient gas pressure effects

The LA plumes expand freely in vacuum. The entire hydrodynamics of plume expansion becomes complex in the presence of a background gas, causing effects such as plume splitting, sharpening, confinement, and the formation of internal plume structures.[20] Computational modeling of ns-LA shock wave propagation in an ambient gas has been achieved and found to match closely with experimental results.[21] Both nature and pressure of the ambient gas affect the plume hydrodynamics and emission features. Also ambient gas environment plays a very important role in plasma spatio-temporal evolution due to plasma plume-ambient species collisional interactions. A higher background pressure will cause the plasma to be confined in a smaller volume, enhancing collisional excitation, which, in turn, leads to an increase in line emission intensity and also higher background emission. The pressure also plays a role in line broadening due to increased electron density with pressure.[20] Fig. 4 shows the spectral emission for a range of pressures at a distance 2 mm from the target and with laser excitation energy 100 mJ. It is important to note here that the vacuum spectrum was obtained with 0 μs delay and 5 μs gate width due to the plasma's rapid expansion and low persistence; the majority of emission in vacuum is seen 0–1 μs. However, the detection of this early time in the plasma leads to an increase in observed background emission. All other spectra were taken with a 1 μs delay and 20 μs integration time.

Fig. 4 shows the spectral intensity and background increased with pressure. The total emission intensity is highest at 100 Torr, as is the line emission intensity. The background-subtracted line intensity and signal to background ratio for the U I 356.18 nm line plotted versus ambient Ar gas pressure are given in Fig. 5. Increased plasma confinement causes the decrease in intensity above 100 Torr; the spectra are taken 2 mm from the target, which is near the edge of plasma expansion above 100 Torr, whereas at 100 Torr, the spectrum is taken from the hot center of the plasma, where line emission is high. Signal to background ratio also follows a similar trend to line intensity, peaking at 100 Torr. Therefore, 100 Torr is the optimal Ar pressure under these conditions and is used as the ambient environment for the other experiments here. Increased pressure causes more collisional effects due to higher density and less ablation/more heating, which leads to more species excitation and background emission.[20]

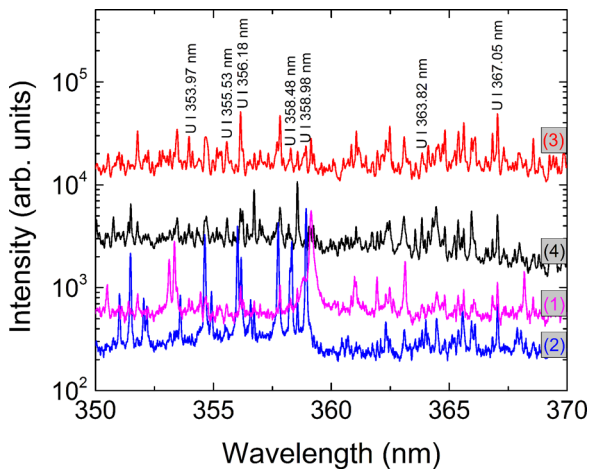

FIG. 4. Spectra obtained at (1) vacuum, (2) 1 Torr, (3) 100 Torr, and (4) 760 Torr, distance 2 mm from target and laser energy 100 mJ. Vacuum (1) spectrum was obtained with 0 μs delay due to low persistence, resulting in increased continuum emission.

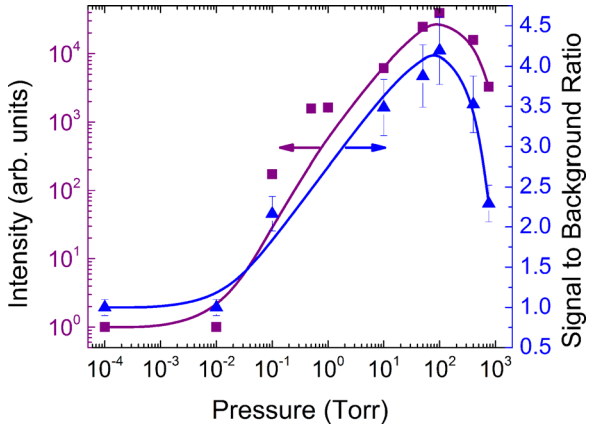

FIG. 5. Intensity and signal to background ratio of the U I 356.18 nm line versus ambient gas pressure, taken 2 mm from the target with laser energy 100 mJ. Intensity and S/B peak for 100 Torr Ar.

C. Spatial plasma emission evolution

The plasma parameters change rapidly with space, and hence the excitation and de-excitation mechanisms are also a function of space. As seen in the 760 Torr spectrum in Fig. 4, spatial evolution of the plasma plays a very important role in spectral emission analysis. Typical spectra obtained at various distances in the spectral range of 350–370 nm, with laser excitation energy of 100 mJ and ambient Ar pressure 100 Torr are given in Fig. 6. In the hot center of the plasma, emission is higher, while the emission decreases near the plasma/gas interface (farther from the target surface) that is sampled.

The plasma/gas interface is evident when examining individual line emission intensity. The background-subtracted

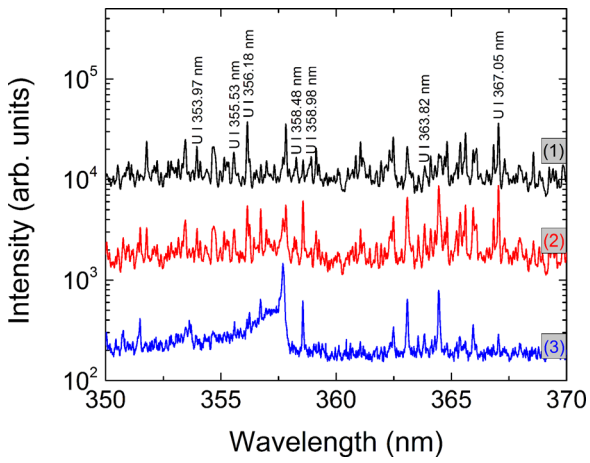

FIG. 6. Spectra obtained at (1) 3 mm, (2) 5 mm, and (3) 7 mm, with laser energy 100 mJ and ambient environment 100 Torr Ar. Continuum emission is more intense closer to the target, as is line emission.

intensity and signal to background ratio of the U I 356.18 nm line were calculated from the spectra in Fig. 6 as a function of distance from the target surface, with laser energy 100 mJ and ambient Ar pressure 100 Torr (Fig. 7). The intensity is approximately constant from the target surface up to 4 mm from the target, and then decreases rapidly until 8 mm from the target, where it begins to level out. Line emission in the 8–10 mm range is negligible, indicating that the plasma/gas interface is near 8 mm from the target. This rapid decrease in line emission intensity is due to plume confinement and reduction in plasma temperature with space.[22] The plasma/gas interface is also observed around 8 mm in the signal to background ratio for the U I line, where the signal intensity completely ceases. The S/B ratio is approximately constant from the target surface to 4 mm from the target and peaks between 4 and 5 mm from the target. The intensity and S/B ratio behavior match well as a function of distance from the target, again indicating that line emission and background emission exhibit similar excitation behaviors. The optimal line emission intensity and S/B ratio are observed in the range of 2 to 5 mm from the target surface.

D. Temporal plasma emission evolution

The temporal evolution of the plasma line emission dictates the optimal time window for optical detection (gate delay and width) and is therefore crucial information, especially for detection of low-concentration elements and/or low-intensity lines. Temporal evolution is also important to understand as to how ambient gas influences persistence of various species in the plasma. Temporal evolution of plasma emission can be investigated using two distinct spectroscopic methods. First, a programmable timing generator (PTG) is coupled to the ICCD camera, providing multichannel detection (i.e., a range of wavelengths); the delay is then varied with a narrow integration time (in this case, the gate width was set to 10% of the delay). Second, the emission is diverted to a PMT instead of the ICCD camera and acts as a monochromator. The diffraction grating is set so that a single wavelength is passed to the PMT with the help of a slit, which is then connected to an oscilloscope, which reads out the intensity of the line emission as a function of time. Both the methods were used here, as each has its advantages. Time-resolved spectra capture a range of wavelengths, which reduce error in correctly identifying the line peak. However, the optical TOF method reduces error associated with the width of the integration time used for time-resolved spectra, as the intensity is taken in real time considering PMT has a rise time <2 ns. Delay and persistence of selected species can be measured with high precision and accuracy using OTOF.

The temporal evolution of the U I 356.18 nm line from time-resolved spectra is given in Fig. 8, with laser energy 100 mJ and Ar pressure 100 Torr. The emission intensity peaks at $\sim 6\,\mu$s after the laser pulse. The line emission also persists for approximately 30 μs; the delay and integration time used for the time-integrated spectra ensure that the peak intensity and majority of the line emission are captured.

The TOF information was also obtained using the PMT for comparison with the time-resolved spectra. The TOF profiles for the U I 356.18 nm line are given in Fig. 9 for various Ar pressure levels recorded at a distance 2 mm from the target surface. The OTOF profiles show significant changes in delay (arrival time), persistence, and intensity with the addition of ambient pressure. The persistence of excited U I is found to be overlapped with background continuum at vacuum and low pressure levels. For example, at 1 Torr, the line emission is barely discernible from the background emission, which is observed as a sharp peak near 0 delay time. However, the emission peak is getting delayed with increasing pressure along with persistence. The presence of a sharp peak at the earliest time even at higher pressures indicates that continuum emission is also responsible for strong background emission in U containing plasmas. The temporal separation between the background emission and excited U I species is evident when the pressure $>\sim 25$ Torr. The peak delay time and line emission decay time (persistence) are obtained from the OTOF profiles as a function of pressure

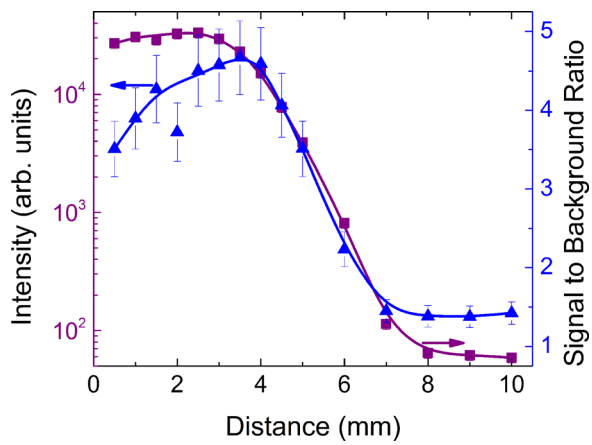

FIG. 7. Intensity and signal to background ratio of the U I 356.18 nm line versus distance from the target, taken with laser energy 100 mJ and ambient environment 100 Torr Ar. Line emission intensity is approximately constant for 0–4 mm from the target, then decreases rapidly.

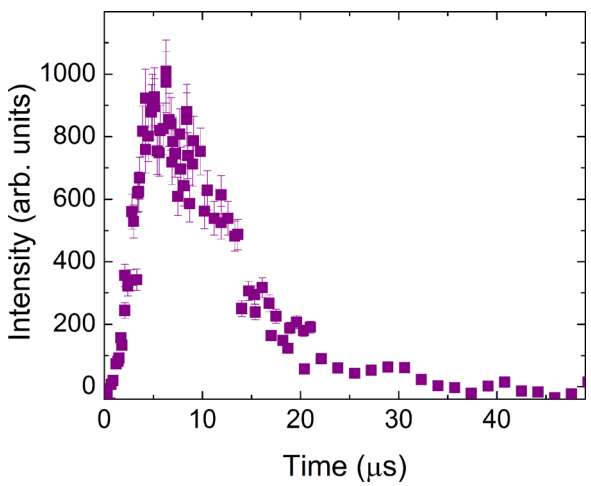

FIG. 8. TOF data from time-resolved spectra for U I 356.18 nm line emission, with gate width 10% of the gate delay. The spectra were obtained with laser energy 100 mJ and ambient environment 100 Torr Ar. Emission peaks for a delay of $\sim 6\,\mu$s.

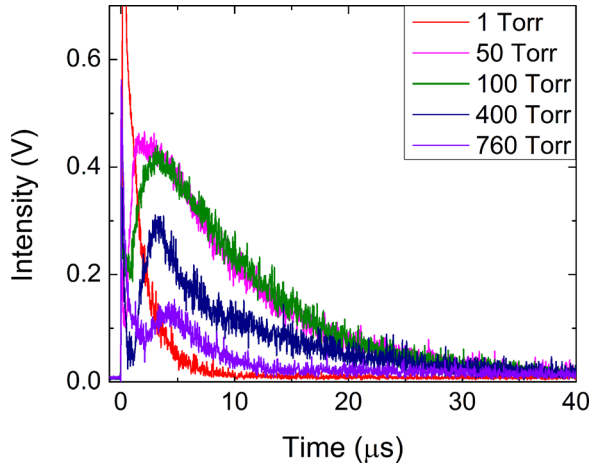

FIG. 9. TOF profiles taken using a PMT for the U I 356.18 nm line versus pressure. Profiles show a peak shift to larger delay times and increase in persistence for higher pressures.

and are given in Figs. 10 and 11, respectively. Delay time increased as a function of ambient pressure from 0.5 to 3 μs due to slowing of plasma species from collisions with the ambient gas; higher backing pressure results in deceleration of plasma species. Plasma emission decay time or plasma persistence, was calculated as where the profile tail falls to $1/e^2$ of the peak intensity. Decay time also increases with ambient pressure, as the plasma confinement increases collisions and therefore the persistence of emission. The persistence data match well with that obtained from the time resolved spectra, though the peak delay time is about half. This could be an effect of the spectral integration time, which can artificially inflate the detected intensity as the integration time increases with delay. The delay time obtained from the OTOF profiles can be used for generating expansion velocities of U I species at various pressure levels and results are also given in Fig. 10. At low pressures, the emission species have a very high velocity, while at higher pressures collisions within the plasma and with the ambient gas slow down the species.

TOF profiles were measured at various distances from the target surface as well to get a better picture of the

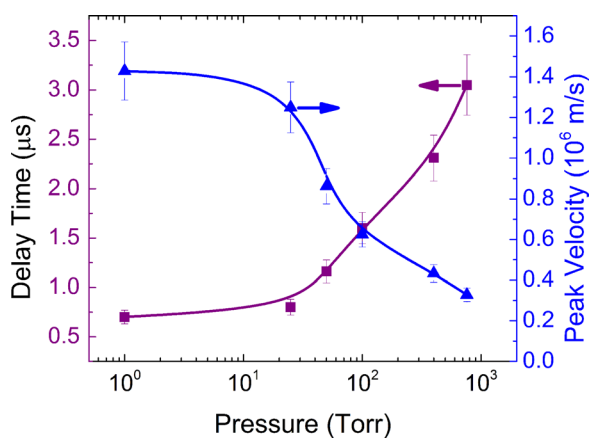

FIG. 10. Peak delay time and peak velocity from TOF profiles as a function of pressure at a distance of 2 mm from the target. Delay time increases and peak velocity decreases with pressure due to plasma collisional effects.

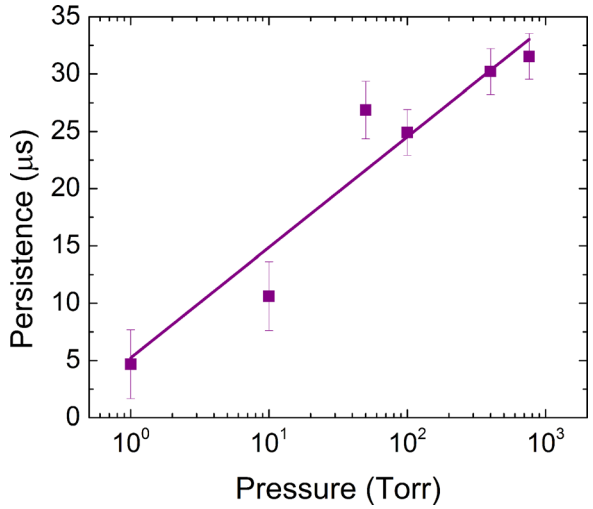

FIG. 11. Emission decay time from TOF profiles as a function of pressure, taken 2 mm from the target. Decay time was calculated from the point, where the plasma intensity is $1/e^2$ of the peak intensity.

temporal evolution of U species at various locations in the plasma, with ambient Ar gas pressure of 100 Torr; typical profiles are given in Fig. 12. As expected, emission intensity decreases with increased distance from the target, and very close to the target, the line emission is difficult to separate from the continuum emission peak. Again the peak delay and velocity (Fig. 13) and line emission persistence (Fig. 14) are calculated from the TOF plots. The peak delay time increases from 1 μs up to 12 μs for distances 1 mm to 6.5 mm from the target; velocity decays rapidly with distance, meaning that the plasma species take time to reach further distances as the plasma expands. Decay time also increases from 20 μs to 38 μs with increased distance from the target. Emission intensity near the target will decrease as the plasma expands into the ambient gas environment, and confinement causes species to reside at further distances for extended duration. Also, species are slowed with increasing distances as can be seen from the peak velocity; these species thus have

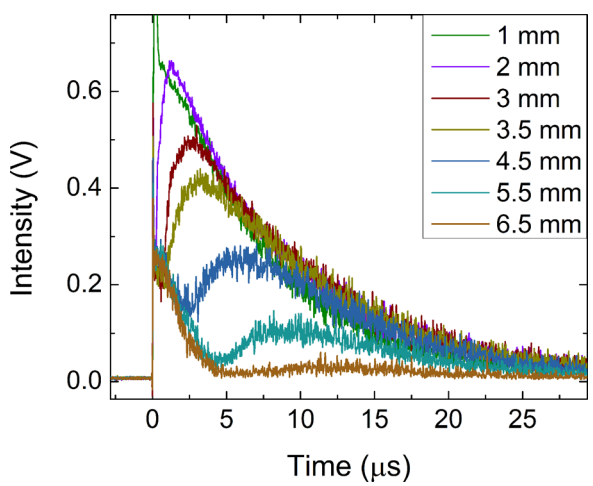

FIG. 12. TOF profiles taken using a PMT for the U I 356.18 nm line versus distance from the target, with laser energy 100 mJ and ambient environment 100 Torr Ar. Peak delay and decay time increase with increased distance from the target.

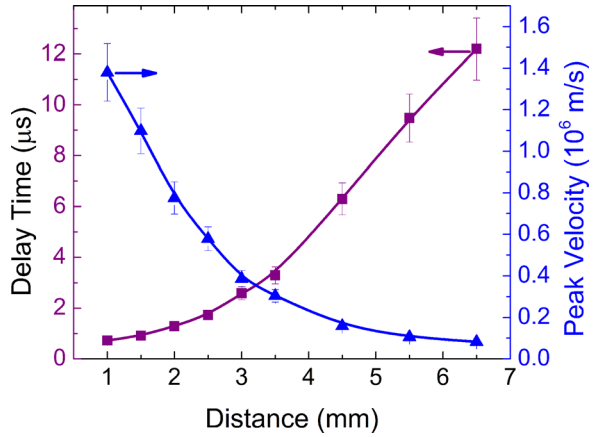

FIG. 13. Peak delay time from TOF profiles as a function of distance from the target, with ambient environment 100 Torr Ar. Delay time increases with distance from the target.

longer residence times at further distances, increasing persistence at those locations.

The TOF profiles obtained using the PMT again indicate that the time settings used for the time-integrated spectra were appropriate. The initial, sharp intense peak from the continuum emission is avoided by using a delay time of 1 μs, while the integration time of 20 μs ensures that the majority, if not all, of the spectral line emission is captured.

Overall, the obtained results indicate that the excitation of U species is collisional and is highly spatial and time dependent. The persistence of U species is limited in vacuum and overlapped with strong background radiation. However, the addition of Ar ambient improved the persistence as well as temporally separated the line emission features from the background. Increased ambient pressure helps to confine the plasma species, increasing particle collisions and enhancing line emission; this is clearly observed in Fig. 5. However, above 100 Torr, line broadening becomes significant,[13,20] causing an overlap in emission lines and increasing the background level of the spectrum; this results in the decrease in background-subtracted intensity seen at pressures above 100 Torr. Plasma persistence also increases as a result of collisional effects, which is a key result for many applications including LIBS, laser absorption spectroscopy and allows for longer spectral integration times.

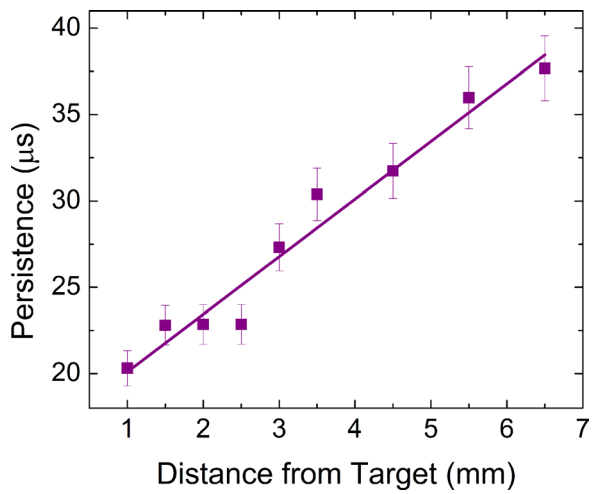

FIG. 14. Emission decay time from TOF profiles as a function of distance from the target, with ambient environment 100 Torr Ar. Decay time was calculated from the point, where the plasma intensity is $1/e^2$ of the peak intensity.

IV. CONCLUSION

We investigated the spatio-temporal evolution of U species in laser-produced plasmas. Improved signal intensity and high persistence of U lines is absolutely necessary for analytical applications. A set of optimal operating conditions was determined based on the results of these experiments, which is important for obtaining the optimal spectral intensity from samples that could contain very small amounts of uranium. Emission intensity tends to approach plateaus for energies 80–120 mJ, indicating that this energy range should be used for Nd:YAG 1064 nm laser as excitation source.

Plasma collisional effects in the presence of ambient gas are the main cause for changes in excitation of various U lines and hence the changes in spectral intensity, with peak intensity found for 100 Torr Ar. Plasma confinement, and thereby the ambient gas pressure, also influences the spatial evolution of the plasma. Emission is approximately constant close to the target, and then decreases rapidly near the plasma/gas interface, which clearly indicates the confinement region. Optical emission detection should be performed within this hot central region to obtain spectra with intense line emission.

Finally, the temporal evolution of the plasma was investigated to find the delay in the peak emission intensity and plasma persistence. These experiments indicate that obtaining spectra with a delay of 1 μs and integration time of 20 μs will capture the majority of the plasma emission, while avoiding the most intense continuum emission immediately after the laser pulse for the conditions used. The persistence of line emission increases with increased pressure due to increased collisional effects, the primary U excitation/de-excitation mechanism; persistence of up to 30 μs is attainable at higher pressures. This investigation of the spatio-temporal evolution of U plasmas provides novel insights into not only the fundamentals of the plasma expansion, but also optimal sampling conditions of U-containing materials. Optimal conditions of 100 Torr Ar, 100 mJ laser energy, with 20 μs spectral integration time sample the plasma emission in the region, where collisional effects greatly enhance line emission and plasma persistence, while avoiding the plasma cooling that occurs at higher pressures due to more collisions.

ACKNOWLEDGMENTS

This work was partially supported by DOE-NNSA and NSF-PIRE.

[1]N. Wogman, J. Radioanal. Nucl. Chem. **296**, 1071 (2013).
[2]R. Kouzes, Am. Sci. **93**, 422 (2005).
[3]N. L. LaHaye, S. S. Harilal, P. K. Diwakar, A. Hassanein, and P. Kulkarni, J. Appl. Phys. **114**, 023103 (2013).
[4]N. L. LaHaye, S. S. Harilal, P. K. Diwakar, and A. Hassanein, J. Anal. At. Spectrom. **28**, 1781 (2013).

[5]N. Taylor and M. Phillips, Opt. Lett. **39**, 594 (2014).
[6]A. Sarkar, D. Alamelu, and S. K. Aggarwal, Talanta **78**, 800 (2009).
[7]J. E. Barefield II, E. J. Judge, J. M. Berg, S. P. Willson, L. A. Le, and L. N. Lopez, Appl. Spectrosc. **67**, 433 (2013).
[8]M. Z. Martin, S. Allman, D. J. Brice, R. C. Martin, and N. O. Andre, Spectrochim. Acta Part B **74–75**, 177 (2012).
[9]E. J. Judge, J. E. Barefield II, J. M. Berg, S. M. Clegg, G. J. Havrilla, V. M. Montoya, L. A. Le, and L. N. Lopez, Spectrochim. Acta Part B **83–84**, 28 (2013).
[10]I. Choi, G. C.-Y. Chan, X. Mao, D. L. Perry, and R. E. Russo, Appl. Spectrosc. **67**, 1275 (2013).
[11]Y.-S. Kim, B.-Y. Han, H. S. Shin, H. D. Kim, E. C. Jung, J. H. Jung, and S. H. Na, Spectrochim. Acta Part B **74–75**, 190 (2012).
[12]E. C. Jung, D. H. Lee, J.-I. Yun, J. G. Kim, J. W. Yeon, and K. Song, Spectrochim. Acta Part B **66**, 761 (2011).
[13]R. C. Chinni, D. A. Cremers, L. J. Radziemski, M. Bostian, and C. Navarro-Northrup, Appl. Spectrosc. **63**, 1238 (2009).
[14]G. C.-Y. Chan, X. Mao, I. Choi, A. Sarkar, O. P. Lam, D. K. Shuh, and R. E. Russo, Spectrochim. Acta Part B **89**, 40 (2013).
[15]D. A. Cremers, A. Beddingfield, R. Smithwick, R. C. Chinni, C. R. Jones, B. Beardsley, and L. Karch, Appl. Spectrosc. **66**, 250 (2012).
[16]F. R. Doucet, G. Lithgow, R. Kosierb, P. Bouchard, and M. Sabsabi, J. Anal. At. Spectrom. **26**, 536 (2011).
[17]K. J. Grant and G. L. Paul, Appl. Spectrosc. **44**, 1349 (1990).
[18]See http://www.pmp.uni-hannover.de/cgi-bin/ssi/test/kurucz/sekur.html for *Atomic Spectral Line Database*, edited by P. L. Smith, C. Heise, J. R. Esmond, and R. L. Kurucz, 2014.
[19]A. E. Hussein, P. K. Diwakar, S. S. Harilal, and A. Hassanein, J. Appl. Phys. **113**, 143305 (2013).
[20]N. Farid, S. S. Harilal, H. Ding, and A. Hassanein, J. Appl. Phys. **115**, 033107 (2014).
[21]S. S. Harilal, G. V. Miloshevsky, P. K. Diwakar, N. L. LaHaye, and A. Hassanein, Phys. Plasmas **19**, 083504 (2012).
[22]B. Verhoff, S. S. Harilal, J. R. Freeman, P. K. Diwakar, and A. Hassanein, J. Appl. Phys. **112**, 093303 (2012).